Heavy ion collisions at intermediate energy

G. Bertsch
Physics Department, Michigan State University, East Lansing, Michigan 48824

A. A. Amsden
Theoretical Division, Los Alamos Scientific Laboratory, Los Alamos, New Mexico 87545
(Received 24 March 1978)

Two types of measurement are proposed for the analysis of heavy ion collisions in the range of energy of 20–200 MeV/A. First, measurement of the longitudinal component of the kinetic energy of the collision products characterizes the impact parameter of the collision. The distribution in this quantity allows the dissipation in the theoretical models to be determined. A second kind of measurement is that of the coefficients of a spherical harmonic expansion of the angular distribution of the products. Besides giving independent information on the impact parameter and reaction dynamics, measurement of these coefficients offers the possibility of measuring the stiffness of the equation of state of nuclear matter. These ideas are explored in the context of a hydrodynamic model for the collision. In the purely hydrodynamic model there is a large measurable asymmetry in the angular distribution, but the dependence on the equation of state is small.

[NUCLEAR REACTIONS Heavy ion collisions. Energy loss and angular distributions discussed and related to dissipation mechanism, equation of state. Hydrodynamic calculations.]

INTRODUCTION

An important motivation for measuring heavy ion collision cross sections at intermediate energy is to study nuclear matter at high density. In particular, we would like to know whether there are any unusual phenomena such as phase transitions, associated with high density nuclear matter. The quantitative goal is to infer information about the nuclear equation of state from the experimental observables.

To date, no clear dependence of experimental observables on the fundamental properties of nuclear matter has been demonstrated. The type of experiment carried out most extensively is the measurement of the energy- and angle-differential cross section for various kinds of collision products,[1] summing over all final states. The theoretical predictions for these measurements have been found to be remarkably insensitive to the theoretical model.[2] The basic problem is that an inclusive cross section measurement averages over the impact parameter of the collisions, and much information is lost. We propose two measurements of energy and angular distribution that involve all of the collision products. While much more difficult to interpret experimentally, we will show below that these quantities can be readily interpreted theoretically.

ENERGY

We propose that the total c.m. kinetic energy in the longitudinal direction be measured for collisions between the equal mass target and the projectile. Nonrelativistically, this can be defined as

$$E_{\parallel} = \sum_i \frac{p_{\parallel}^2(i)}{2m_i}, \tag{1}$$

where the sum is over all collision products, and $p_{\parallel}(i)$ is the momentum of the ith particle along the beam direction. The experimental measurement will give a probability distribution in $E_{\parallel}$, which we call $dN/dE_{\parallel}$. The value of $E_{\parallel}$ for a particular collision will correlate with the impact parameter; the point at which $dN/dE_{\parallel}$ goes to zero will correspond to head-on collisions. The value of $E_{\parallel}$ at the small impact parameters is quite dependent on the model of the collision, the variation depending on how quickly the coherent motion of the two heavy ions coming together is converted to thermal energy by nucleon-nucleon collisions.

One extreme is the hydrodynamic model, in which the pressure tensor is assumed to be isotropic. In this situation, the nuclear matter is sprayed out in the transverse direction when there is a head-on collision. Thus $E_{\parallel}$ will be quite small for these collisions. We illustrate this with numerical 3-D hydrodynamic calculations. The calculation scheme and other results are described in Ref. 3. We consider collisions of mass 40 nuclei, at energies of 100 MeV/A (lab) and 400 MeV/A (lab), using the same equation of state as in Ref. 3. In Fig. 1 we show the longitudinal energy fraction as a function of impact parameter. We see that there is not a significant difference between the two energies. In Fig. 2 we plot the

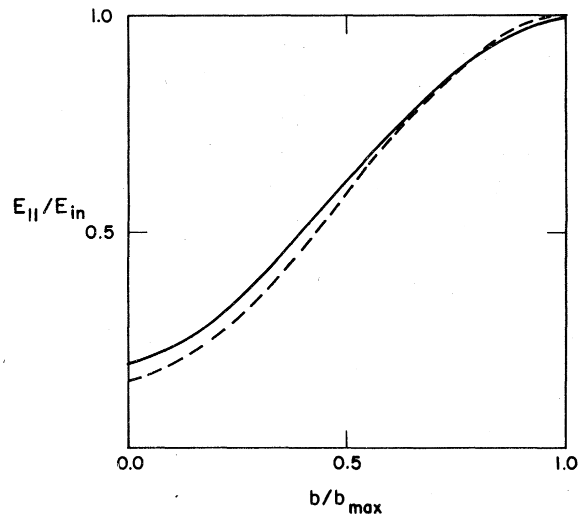

FIG. 1. Longitudinal energy fraction, Eq. (1), as a function of impact parameter, in the hydrodynamic model. The collision is between two mass 40 nuclei, with a bombarding energy of 400 MeV/A (lab) for the solid line and 100 MeV/A for the dashed line.

energy function distribution according to

$$\frac{dN}{dE_{\parallel}} \sim b\frac{db}{dE_{\parallel}}. \qquad (2)$$

The intercept gives the minimum energy fraction and has a value of 0.15–0.2. This substantiates the earlier statement that in the hydrodynamic model the motion is largely converted to the transverse direction.

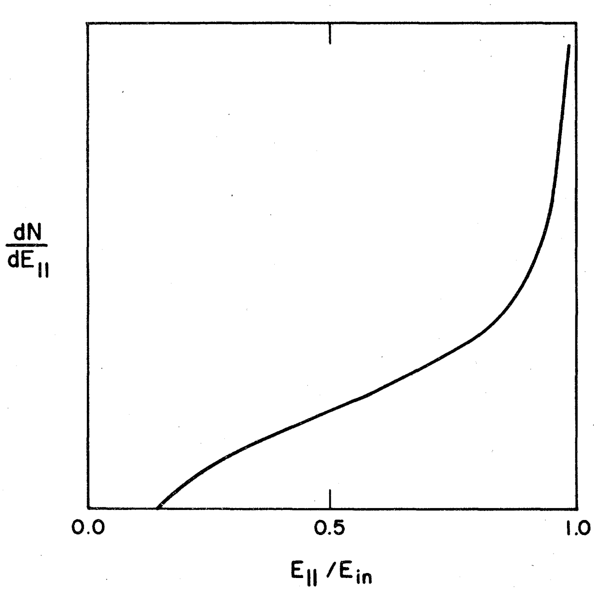

FIG. 2. Probability distribution for the longitudinal energy fraction in the hydrodynamic model, Eq. (2). The collision parameters are given in the caption to Fig. 1.

A model that has been useful in interpreting the single-particle cross sections is the "fireball model."[1] Here it is assumed that the colliding matter produces an isotropic thermal distribution in the region of overlaps of the two ions. The head-on collisions in this model would obviously have a longitudinal energy fraction of

$$E_{\parallel}/E_{in} = \tfrac{1}{3}.$$

While the single-particle data at 400 MeV/A is consistent with the model, the cross sections at relativistic energies show a lesser degree of thermalization. Thus, one would expect the longitudinal energy fraction to be larger than $\frac{1}{3}$ at the highest energies.

Finally, the mean-field models, exemplified by time-dependent Hartree-Fock theory, have very small dissipation. Only the mean potential field mediates the dynamics, giving very little conversion of kinetic energy from the longitudinal to the transverse directions. At low energies, the collision is capable of absorbing energy by lowering the density of the system; at 5 MeV/A the longitudinal fraction in the collision of thick slabs is 0.13.[4] However, the amount of energy that can be absorbed this way is bounded by the total potential interaction energy. As the bombarding energy is increased, the effect of the mean field becomes weaker and the longitudinal fraction should approach 1.

ANGULAR DISTRIBUTIONS

Again, let us consider only collisions between equal mass target and projectile, and work in the c.m. frame. We consider that the angles of many particles have been measured and define an angular distribution by a fit to the spherical harmonic expansion

$$f(\theta,\phi) \sim Y_0 + \sum_{M}^{L>0} \alpha_{LM} Y_M^L(\theta,\phi). \qquad (3)$$

Details of defining such an expansion and the statistical uncertainty in the coefficients, are given in the Appendix. We need only consider even L by the symmetry. Let us truncate the expansion at $L=2$ and consider only the behavior of the coefficients α_{2M}. The symmetry with respect to inversion in the reaction plane will reduce the number of independent coefficients to three; assuming the reaction to be in the xz plane, these are

$$\alpha^{(0)} = \alpha_{20},$$

$$\alpha^{(1)} = \frac{1}{\sqrt{2}}(\alpha_{21} - \alpha_{2-1})$$

$$\alpha^{(2)} = \frac{1}{\sqrt{2}}(\alpha_{2,2} + \alpha_{2,-2}).$$

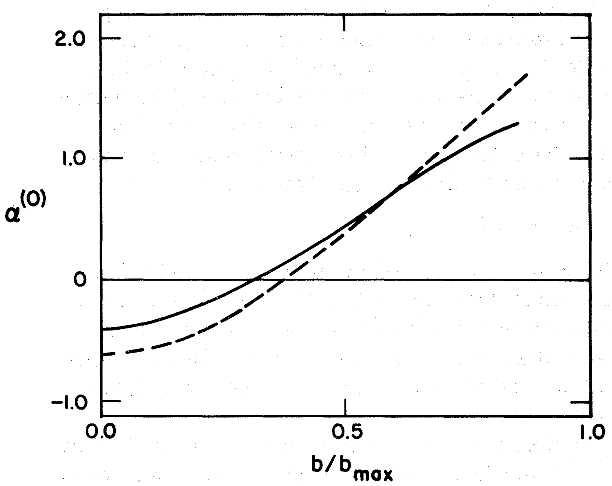

FIG. 3. Angular distribution coefficient $\alpha^{(0)}$ for low-energy particles ($E<\frac{1}{2}E_{in}$) emerging from heavy ion collisions, as a function of impact parameter. Solid and dashed lines are as in caption to Fig. 1. The coefficient becomes ill determined at the maximum impact parameter, since the number of low-energy particles approaches zero.

We now discuss the qualitative behavior to be expected for the coefficients $\alpha^{(i)}$. The coefficient $\alpha^{(0)}$, measuring the prolateness or oblateness of the angular distribution, is closely connected with the longitudinal energy fraction. For the head-on collisions, $\alpha^{(0)}$ will be negative in the hydrodynamic limit and positive in the mean-field limit. In Figs. 3 and 4 we show the predicted $\alpha^{(0)}$ for the hydrodynamic calculations described previously. Figure 3 sums the low-energy particles $E<\frac{1}{2}E_{in}$ and Fig. 4 shows the distribution for particles with energy near the beam energy. There is not much dependence on bombarding energy, or on the energy of the group of particles measured in the final state.

The coefficients $\alpha^{(1)}$ and $\alpha^{(2)}$ of course must vanish for head-on collisions, by the azimuthal symmetry. At intermediate impact parameters, there will be asymmetry resulting from several physical effects. Consider a collision at large impact parameter, at the moment of maximum overlap of the two nuclei. There is a high-density, high-temperature overlap region which gives rise to a transverse force between the nuclei. This force is transmitted to each nucleus as a whole, and so we should expect a deflection of the residual fragments. This would show up as a non-vanishing $\alpha^{(1)}$ coefficient for fragments having the same energy as the incoming energy. Thus the $\alpha^{(1)}$ coefficient is determined by the transverse pressure. The pressure of course is directly related to the equation of state, depending on the thermal energy and the density-dependent potential field. Knowledge of the dissipation dynamics tells us the thermal component of the pressure; the remainder comes from the density dependence of the equation of state and can be inferred. In Figs. 5 and 6 we display the predicted $\alpha^{(1)}$ coefficients for the low- and mid-energy groups. The wide variation of $\alpha^{(1)}$, from 0 to ~1 means that a significant measurement may be possible even in single collisions.

To identify the impact parameter for these measurements, the longitudinal energy loss could be used as the independent variable. If the coefficient $\alpha^{(1)}$ were plotted as a function of $E_{\parallel}$, the data

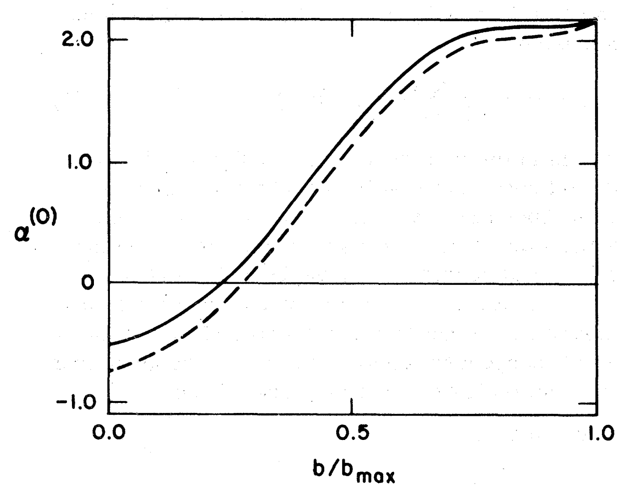

FIG. 4. Angular distribution coefficient $\alpha^{(0)}$ for medium-energy particles ($0.8E_{in}<E<1.2E_{in}$), as a function of the impact parameter. Solid and dashed lines are as in the caption to Fig. 1.

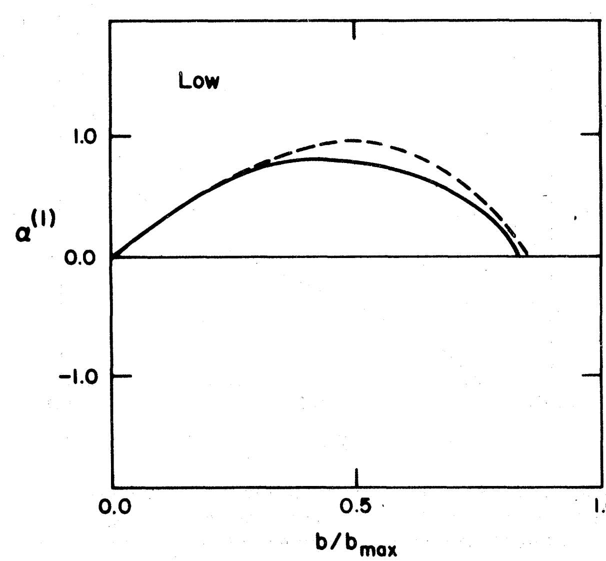

FIG. 5. Same as Fig. 3, for the coefficient $\alpha^{(1)}$.

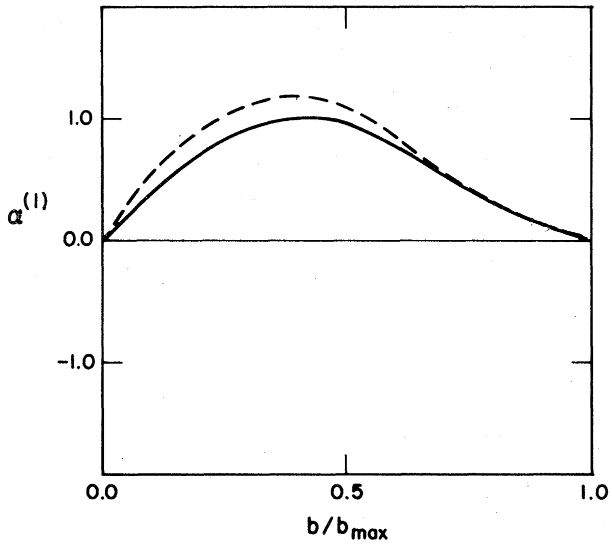

FIG. 6. Same as Fig. 4, for the coefficient $\alpha^{(1)}$.

points should fall along a curve. For the 100 MeV/A hydrodynamic calculation, this curve is shown in Fig. 7. The largest and smallest impact parameters are associated with the maximum and minimum $E_{\parallel}$, and the curve reaches $\alpha^{(1)}=0$ at these points. The nonvanishing $\alpha^{(1)}$ occurs at intermediate $E_{\parallel}$. The experimental data would be individual points in the $(\alpha^{(1)}, E_{\parallel})$ plane, and the density of these points would define a ridge. The information about the average behavior of the colliding system would be reduced to locating this

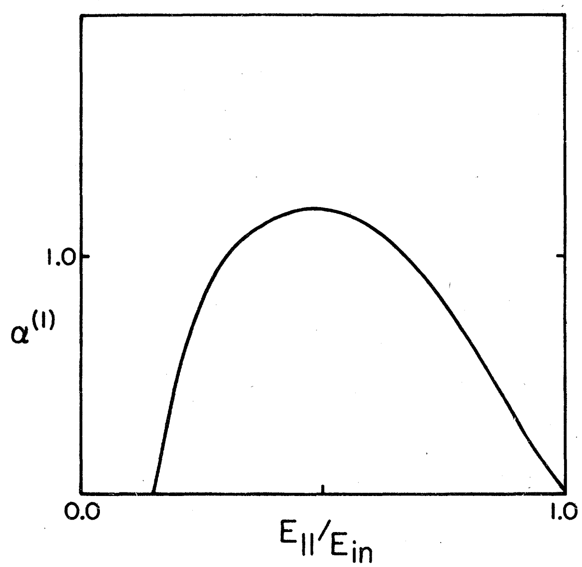

FIG. 7. Variation of the asymmetry coefficient $\alpha^{(1)}$ with the energy loss $E_{\parallel}$. The curve is shown for the 100 MeV/A (lab) collision of two mass 40 nuclei.

ridge. This is similar to a procedure used in the analysis of low-energy collisions, except that for low energies the nuclei remain whole and the measurement is of the energy loss and angular deflection of an individual nucleus.

Finally, we consider the physical effects giving rise to a coefficient $\alpha^{(2)}$. The particles that are emitted from the overlap region will be partly shielded by the nuclei. The particles will preferentially escape in the direction perpendicular to the line of centers; this will give rise to a negative $\alpha^{(2)}$. The abraded nuclei will also emit particles, but here the direction will be preferentially perpendicular to the angular momentum vector, thus in the reaction plane. This gives rise to a positive $\alpha^{(2)}$. In the numerical hydrodynamic calculations, we do not find any systematic trend for $\alpha^{(2)}$. It has a small magnitude, and varies in sign depending on energy group and impact parameter. Thus the $\alpha^{(0)}$ and $\alpha^{(1)}$ are the most promising for future study.

Since these measurements are intended to reveal information about the nuclear matter equation of state, it is of interest to study the dependence of the quantities $\alpha^{(1)}$ and $E_{\parallel}$ on the compressibility modulus. In the above calculation, the assumed model had a compressibility modulus $K=300$ MeV at nuclear matter density. We varied this in the range 200–550 MeV, by changing the parametrization of the equation of state. The effect on $\alpha^{(1)}$ and $E_{\parallel}$ was slight. Evidently, the assumption that the pressure tensor be isotropic is sufficiently strong that any remaining details of its dependence on density are lost. During the collision, the pressure must be strong enough and act for a sufficient duration to bring longitudinal component of momentum to zero, for nucleons in the overlap region. The transverse pressure is just related to this by a geometric factor, and so the transverse momentum transfer will be governed by the longitudinal momentum, with little dependence on the details of the densities. To the degree that the pressure tensor is not isotropic, the transverse momentum transfer will be independent of the longitudinal momentum transfer, and thus sensitive to the equation of state.

This work was done at Los Alamos Scientific Laboratory under the auspices of the U. S. Department of Energy; G. B. also acknowledges support of the National Science Foundation.

APPENDIX

We here examine the uncertainty in the measurement of the distribution function when the angles of N particles are measured. We first characterize the distribution function for this measurement

TABLE I. Variance σ_M from Eq. (6) for distribution functions of the form $F = a(Y_0 + \alpha_0 Y_{20})$.

	σ_0	σ_1	σ_2
$\alpha_0 = 2/\sqrt{5}$	0.88	1.13	0.65
$\alpha_0 = 0$	1.00	1.00	1.00
$\alpha_0 = -1/\sqrt{5}$	0.71	0.92	1.13

as

$$F_{\exp}(\hat{p}) = \sum_i^N \delta(\hat{p} - \Omega_i), \tag{4}$$

where Ω_i are the angles of the particles. This is fitted to the form Eq. (2) by equating the two expressions and integrating with $Y_L(\hat{p})$. We find for the coefficients,

$$\alpha_M^{\exp} = \frac{\sqrt{4\pi}}{N} \sum_i^N Y_{2M}(\Omega_i). \tag{5}$$

The coefficient $\alpha^{\exp}$ is simply an average over the N particles, and therefore the usual statistics will be obeyed. In particular, the uncertainty in $\alpha_M^{\exp}$ is given by

$$\delta\alpha = \langle(\alpha_M^{\exp} - \alpha_M)^2\rangle^{1/2} = \frac{\sigma_M}{\sqrt{N}}, \tag{6}$$

where σ_M is the dispersion in $Y_{2M}(\Omega_i)$, i.e.,

$$\frac{\sigma_M^2}{4\pi} = \frac{\int |Y_{2M}|^2 F(\hat{p}) d\hat{p}}{\int F(\hat{p}) d\hat{p}} - \left(\frac{\int Y_{2M} F(\hat{p}) d\hat{p}}{\int F(\hat{p}) d\hat{p}}\right)^2. \tag{7}$$

In order to measure the distribution function for a single collision, it is crucial that the statistical uncertainty in Eq. (7) be small. From Eq. (6), we see that this depends on the function F.

We now determine the uncertainty under some simple assumptions about F. If only α_0 in Eq. (1) is nonvanishing, we can evaluate Eq. (6) as

$$\begin{aligned} \sigma_0^2 &= (1 + \tfrac{2}{7}\sqrt{5}\,\alpha_0 - \alpha_0^2), \\ \sigma_1^2 &= [1 + (\sqrt{5}/7)\alpha_0], \\ \sigma_2^2 &= (1 - \tfrac{2}{7}\sqrt{5}\,\alpha_0). \end{aligned} \tag{8}$$

The requirement that F be non-negative limits α_0 to the range

$$-1/\sqrt{5} \leq \alpha_0 \leq 2/\sqrt{5}. \tag{9}$$

We evaluate σ_M for distribution functions in this range, with the results shown in Table I. There is some variation in σ with α_0, confirming the intuitive expectation that the distribution should be more easily measured as it becomes more localized. Let us assume now that the distribution function is oblate for central collisions, and examine the uncertainty in α_1, which ought to be nonzero only for noncentral collisions. If 10 particles are measured, Eq. (6) yields an uncertainty $\delta\alpha_1 \approx 0.3$, which is substantially less than the range expected for α_1 in the hydrodynamic model.

[1]J. Gosset *et al.*, Phys. Rev. C 16, 629 (1977); G. D. Westfall *et al.*, Phys. Rev. Lett. 37, 1202 (1976).
[2]A. Amsden, *et al.*, Phys. Rev. Lett. 38, 1055 (1977).
[3]A. Amsden, F. H. Harlow, and J. R. Nix, Phys. Rev. C 15, 2059 (1977).
[4]P. Bonche, S. Koonin, and J. W. Negele, Phys. Rev. C 15, 2059 (1977).